Available online at www.sciencedirect.com

ScienceDirect

Procedia Engineering 154 (2016) 441 – 449

Procedia Engineering

www.elsevier.com/locate/procedia

12th International Conference on Hydroinformatics, HIC 2016

Effects of morphological change on fluvial flood patterns evaluated by a Hydro-geomorphological model

Jingming Hou[a,b,*], Zhanbin Li[a], Qiuhua Liang[b], Guodong Li[a], Wen Cheng[a], Wen Wang[a], Run Wang[a]

[a]*School of Water Resources and Hydro-power Engineering, Xi'an University of Technology, NO.5 Jinhuan Road, Xi'an, Shaanxi, 710048, China*
[b]*School of Civil Engineering and Geosciences, Newcastle University, Newcastle upon Tyne, NE1 7RU, UK*

Abstract

High aggradation and degradation in a river induced by last flood event will respectively raise and decrease the risk of an upcoming flood event. However, this point is likely to be ignored or is not fully considered in some 2D fluvial flood models. To address this problem, this work develops a 2D high-resolution hydrodynamic model coupled with the sediment transport and the river bed evolution models. The modelling system is within the framework of a Godunov-type finite volume scheme. GPU technique is applied to accelerate the computation by more than 10 times, comparing to the CPU counterpart. After being validated against an experimental benchmark test, the model is applied to simulate the effects of the morphological change on flood patterns for the Bayangaole Reach of Yellow River, China. The results indicate that the effect of perturbed bed could be of significance for the fluvial flood over movable bed. It is therefore suggested to take into account when evaluating the flood risk in this case.

Peer-review under responsibility of the organizing committee of HIC 2016

Keywords: Sediment transport model; Morphological change; Fluvial flood; Shallow water equations; GPU

* Corresponding author. Tel.: +86-15809283371; fax: +86-029-83239907
E-mail address: jingming.hou@xaut.edu.cn

Peer-review under responsibility of the organizing committee of HIC 2016
doi:10.1016/j.proeng.2016.07.536

1. Introduction

Morphological change is of importance for fluvial flood, especially for the rivers with relatively high sediment concentration and movable bed, e.g. the Yellow River in China. The aggraded flood plain could raise the flood risk, causing immeasurable losses to the lives and property. On the contrary, the degraded river bed is likely decrease the water surface level and reduce the flood risk. To reliably predict the flood risk, the morphological effects should be considered. Hydrodynamic models play a significant role in quantitatively evaluate the flood risk, e.g. those in [1-3]. The models are able to model the flood propagation and inundation, however, the river bed evolution is not taken into account. Guan et al. [4] developed a coupled hydro-geomorphological model which could compute the complex solid-fluid interaction process. The model combined with shallow water theory and a non-equilibrium assumption for sediment transport, aiming at simulating the morphological change caused by sediment-laden flows with various sediment transport modes. The modelling concept is applied in this work to develop a GPU based hydro-geomorphological model. The proposed model is validated against an experiment and then adopted to evaluate the morphological effects on the flood propagation and inundation, in order to show the flood pattern may be very different with that of a previous flood with a similar hydrograph, due to the perturbed topography.

2. Governing Equation and Numerical Schemes

The numerical model is governed by the shallow water equations coupled with the sediment transport and bed evolution equations:

$$\frac{\partial \boldsymbol{q}}{\partial t}+\frac{\partial \boldsymbol{f}}{\partial x}+\frac{\partial \boldsymbol{g}}{\partial y}=\boldsymbol{S},$$

$$\boldsymbol{q}=\begin{bmatrix}\eta\\ q_x\\ q_y\\ hC_s\\ hC_b\\ zb\end{bmatrix},\boldsymbol{f}=\begin{bmatrix}q_x\\ uq_x+gh^2/2\\ uq_y\\ q_xC_s\\ \beta q_xC_b\\ 0\end{bmatrix},\boldsymbol{g}=\begin{bmatrix}q_y\\ vq_x\\ vq_y+gh^2/2\\ q_yC_s\\ \beta q_yC_b\\ 0\end{bmatrix},$$

$$\boldsymbol{S}=\begin{bmatrix}0\\ S_{bx}+S_{fx}\\ S_{by}+S_{fy}\\ E_s-D_s\\ E_b-D_b\\ \dfrac{D-E}{1-p}\end{bmatrix}=\begin{bmatrix}0\\ -\dfrac{gh\partial z_b}{\partial x}-C_fu\sqrt{u^2+v^2}\\ -\dfrac{gh\partial z_b}{\partial y}-C_fv\sqrt{u^2+v^2}\\ \varpi_0(C_{sae}-C_{sa})\\ -\dfrac{(q_xC_b-\beta q^*)}{L}\\ \dfrac{1}{1-p}\left[\alpha\left(\dfrac{q_xC_b-q^*}{\beta L}\right)+\varpi_0(1-\alpha)(C_{sa}-C_{sae})\right]\end{bmatrix}.$$

Where, $\boldsymbol{q}$ is the variable vector consisting of the water level η, q_x and q_y (unit-width discharges in the x- and y-direction), hC_s and hC_b (conservative concentration of suspended load and bed load, respectively) and bed elevation z_b; h denotes the water depth following the relationship of $\eta = z_b + h$; $\boldsymbol{f}$ and $\boldsymbol{g}$ are the flux vectors in the x- and y-directions, respectively; u and v are the velocity components in the two Cartesian directions and $q_x = uh$, $q_y = vh$; g represents the gravity acceleration with a value of 9:81 m/s^2; $\boldsymbol{S}$ is the source vector; S_b and S_f are the source term of bed and friction, respectively; D and E denote the deposition and entrainment rates, respectively, and the subscripts s and b are suspended load and bed load, respectively; C_f is the bed roughness coefficient controlled by the Manning coefficient n and water depth in the form of $C_f = gn^2/h^{1/3}$. Regarding the sediment parameters, ϖ_0 is the settling velocity of single sediment particles; C_{sa} means the near-bed concentration at the reference level

of a; C_{sae} represents the near-bed equilibrium concentration at the same reference level, computed by the function of Smith and McLean [5] in this work; β denotes the difference of the velocities of the sediment phase and the fluid water; q^* is the unit-width sediment transport capacity evaluated by the Meyer Peter and Müller equation; L is the non-equilibrium adaptation length of sediment transport; p is the porosity of the bed material; α is the weight coefficient of sediment types. Most of the sediment parameters are determined via empirical formula.

The governing equations above are numerically solved by a Godunov-type finite volume model as presented in other papers of the authors, e.g. [6, 7]. In this model, the Harten, Lax and van Leer approximate Riemann solver with the contact wave restored (HLLC) is applied to compute the numerical fluxes of water, momentum and sediment across cell interfaces. The required face values of the flow and sediment variables are evaluated by using the MUSCL scheme to achieve second order accuracy. They are also reconstructed by using a non-negative depth reconstruction method to preserve the conservation-property (C-property) [6]. The slope source terms are evaluated by the slope-flux method proposed in [6]. The friction source terms are computed using a splitting point-implicit method as in [8]. The time marching is achieved by using a two-stage explicit Runge-Kutta time-integration scheme. To handle the problem of the numerical instabilities caused by the wetting and drying over complex topography, the approach presented in [7] is adopted. It should be mentioned that the hydrodynamic and sediment transport governing equations are solved in a fully coupled way. The numerical model is programmed by applying the CUDA code which could considerably accelerate the computation on GPUs (Graphic Processing Units) [3], aiming to release the computational burden for practical large-scale applications with relatively high resolution. In this work, a desktop with a NVIDIA GeForce GTX 980Ti GPU is used to run all simulations.

3. Model validation and applications

3.1. Model validation

An experimental test investigated in the laboratory of UCL in Belgium [9] is reproduced to verify the capability of the current model in simulating the hydro-geomorphological processes induced by a dam break. As shown in [9], the initial still water depths before and after the gate located at $x = 3.5$ m are 0.25 m and 0 m, respectively, within a domain of 6 m and 0.5 m in *x*- and *y*-directions. A 0.1 m thick movable bed consists of saturated bed sand with a median diameter of 1.72 mm. The Manning coefficient is assumed to be 0.023 as suggested in [4, 9]. The computational domain is discretized into 120,000 squared cells with the size of 0.005m. Courant number is 0.4 for all the simulations.

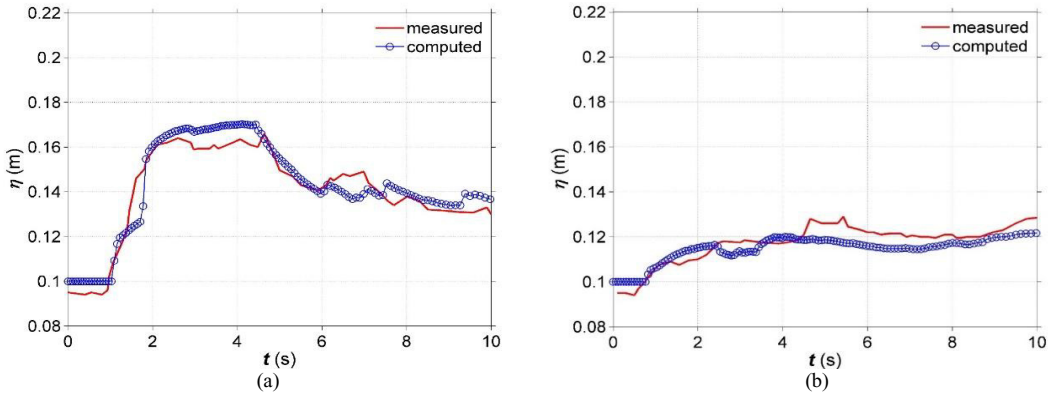

Fig. 1. Computed and measured water levels at (a) Gauge 1; (b) Gauge 2.

As plotted in Figure 1, the computed water levels at Gauges 1 [4.20, 0.375] and 2 [4.70, 0.375] are compared with the measured ones. A good agreement indicates the model can reliably predict the flows over the erodible bed. Besides, the morphological change is simulated as well as shown in Figure 2. In this figure, the modelled bed elevation at $t = 1$ s and 10 s. A pit and a sand bar can be clearly observed between the part of $y = 4$ m and 5 m, in

consistence with that in [4, 9]. The computed bed after flush is also compared with the available measured ones at the cross sections of $y = 4.3$ m and 4.5 m. As plotted in Figure 3, the trend of bed change is correctly evaluated by the current model, confirming the model is able to predict hydro-geomorphological problems caused by flow over erodible bed. The computational time for this test case on GPU and CPU is 312.7 s and 4883.6 s, respectively, i.e. the GPU can accelerate the computation by 15.6 times.

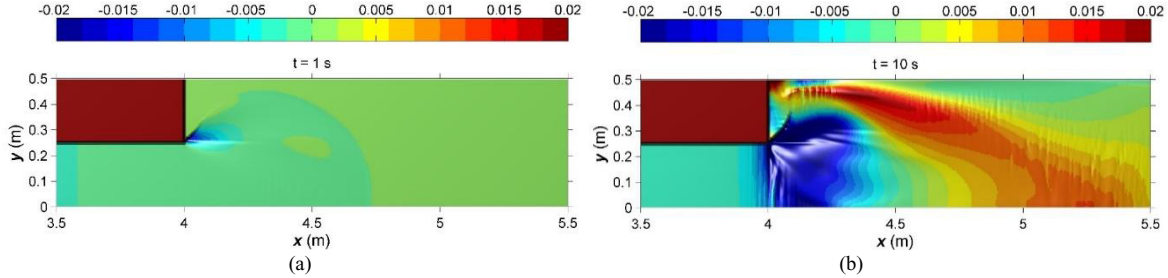

Fig. 2. Computed bed change comparing to the original bed at (a) $t = 1$ s; (b) $t = 5$ s.

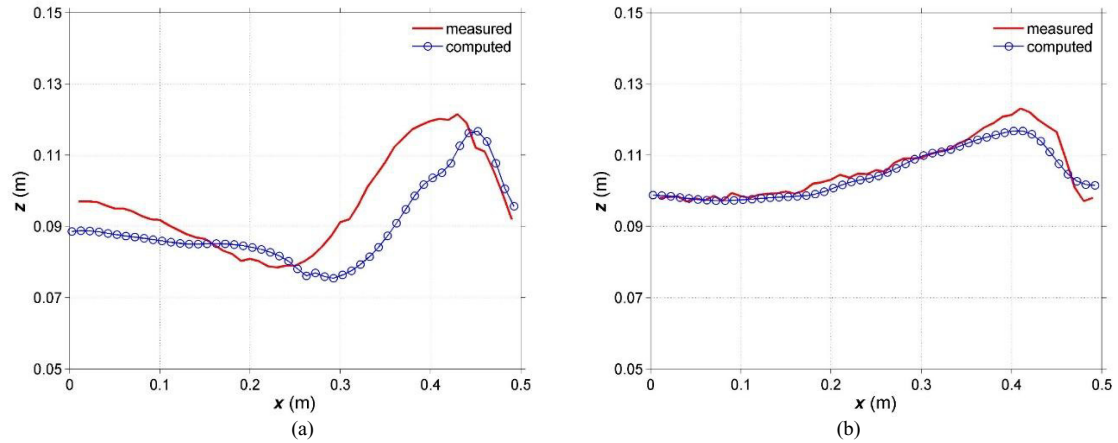

Fig. 3. Computed and measured beds at the cross sections of (a) $y = 4.3$ m; (b) $y = 4.5$ m.

3.2. Application to Bayangaole Reach of Yellow River

In this section, the proposed model is used to investigate the morphological dynamics in the Bayangaole reach of Yellow River, China, during a real flood event in 2002 and a fictive one with the same hydrograph. The inflow hydrograph and the initial bed elevation are sketched in Figure 4. The flood enters the domain from south to north, i.e. the inflow boundary is located at the lower part of the domain (Figure 4(b)). The reach is about 15 km long and 1 km wide and consists of 66,511 squared cells with the size of 30 m. The river banks are assumed as closed boundaries and the north boundary is set as open. The median diameters of the suspended load and bed load are respectively considered as 0.05 mm and 0.18 mm. 0.015 and 0.0017 are imposed at the inflow boundary for the volumetric concentration of the suspended load and bed load, respectively, equivalent to about 40 kg/m^3 and 4.5 kg/m^3 in weight concentration. A constant Manning coefficient is adopted as 0.02. The initial condition is achieved by running the model under the condition of a constant inflow discharge of 1000 m^3/s and fixed bed until reaching a steady stage. Then the model is run for 300 h with the hydrograph plotted in Figure 4(a) and a constant discharge of 1000 m^3/s for 500 h longer to simulate the river recovery process.

Figure 5 plots the morphological change over 300 h and scour is observed in the middle reach. This feature is also sketched in Figure 6 which shows the computed bed change comparing to the original one. The positive values means deposition and negative ones denotes the erosion. It is clearly observed that the deposition and erosion respectively occur in the lower reach (north part) and middle reach. Figure 7 depicts the evolution of the computed water depth, indicating the water depth becomes larger and larger in the middle reach due to scour. It also shows the river starts to be more and more braided in the lower reach.

After 800 h, the new bed is used as initial bed for an upcoming flood event, in order to quantitatively evaluate the effects of the morphological change. The new initial bed is almost the same as that in the left subfigure in Figure 8. The following flood lasts for 300 h with the same inflow hydrograph plotted in Figure 4(a). Figures 8 and 9 sketch the morphological change process. An overall erosion pattern is observed except for the part close to the outlet. It is slight different with the previous event. Figure 10 shows the computed water depth at $t = 100$ h, 200 h and 300 h, indicting the river becomes deeper in the middle reach and more braided in the lower reach. This feature is also plotted in Figure 11 at two cross section of $y = 4497$ km and 4505 km. The computed water levels and bed for the two flood events are compared in Figure 11, illustrating that the water surface level becomes lower in the following flood event due to bed erosion. It also indicates that the flood risk remarkably decreases for the following flood event in this reach, i.e. a flood with a similar hydrograph may cause very different propagation and inundation patterns due to morphological change.

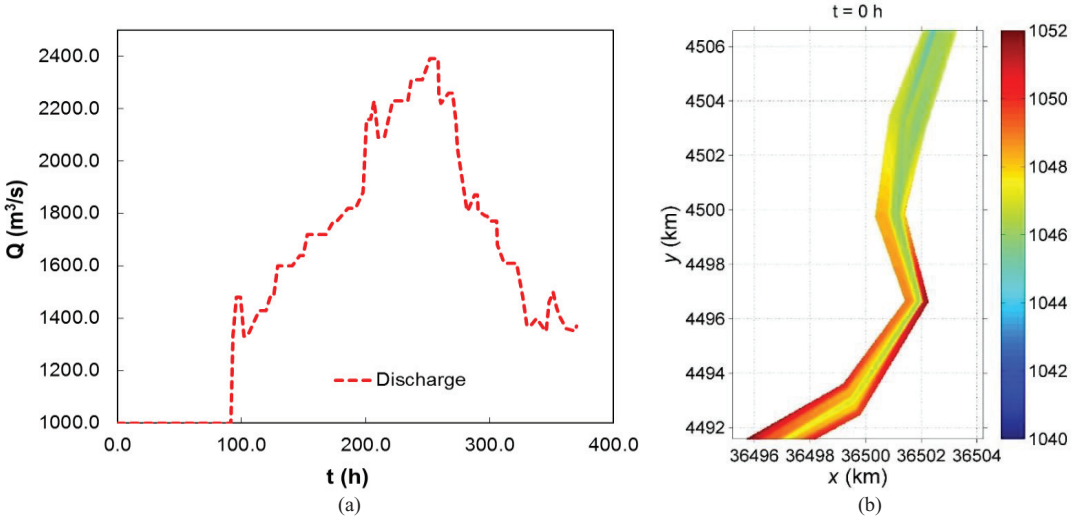

Fig. 4. Inflow hydrograph (left) and the initial bed elevation (right) at the Bayangaole Reach of Yellow River.

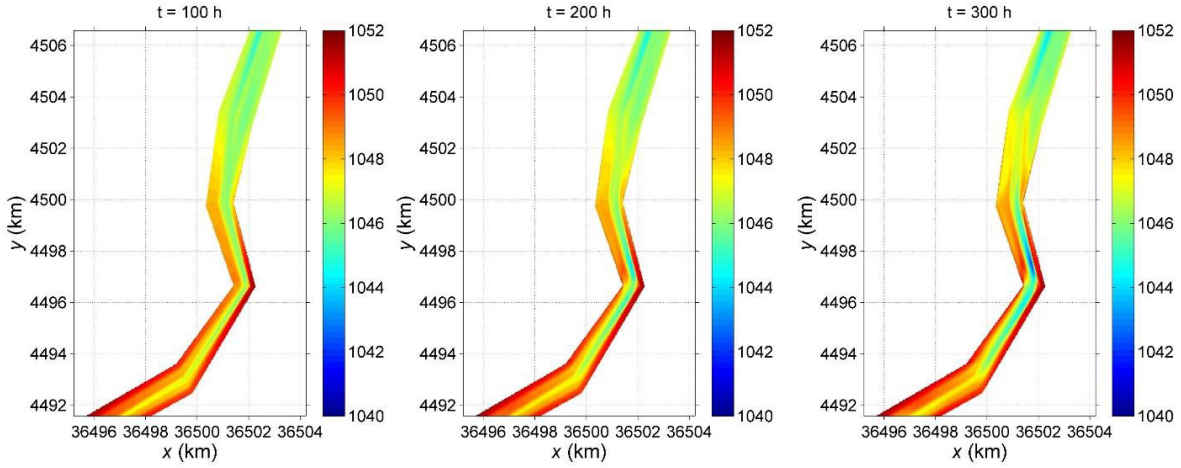

Fig. 5. Computed bed evolution at the Bayangaole Reach of Yellow River.

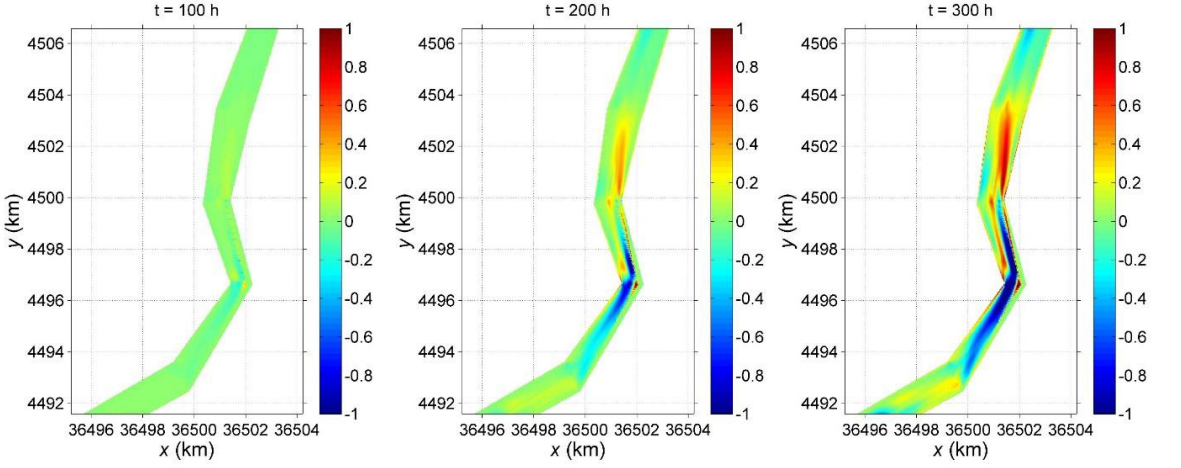

Fig. 6. Computed bed change comparing to the original one at the Bayangaole Reach of Yellow River.

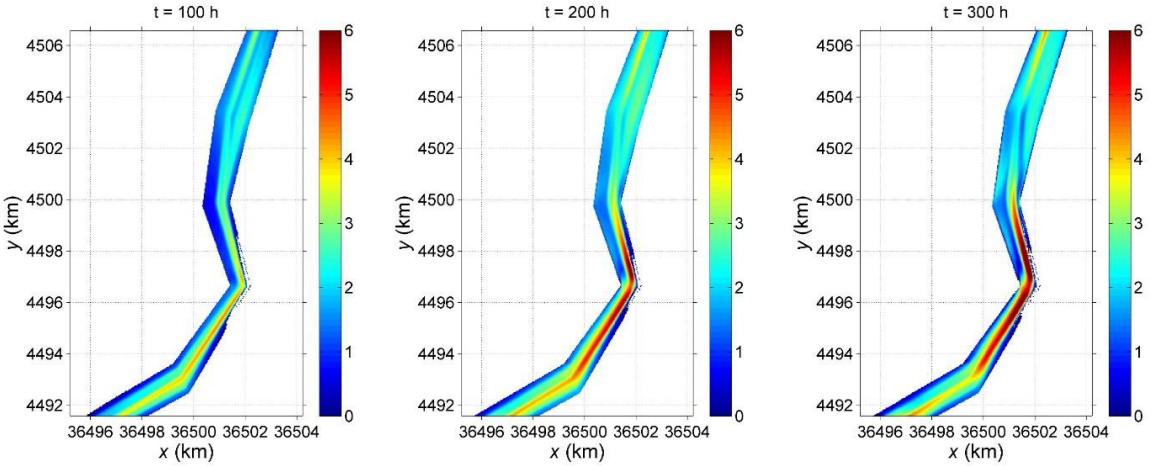

Fig. 7. Computed water depth evolution over the movable bed at the Bayangaole Reach of Yellow River.

4. Conclusions

In this work, a GPU based hydro-geomorphological model is developed and validated against an experiment benchmark test. The model is adopted in the Bayangaole Reach of Yellow River to quantitatively evaluate bed evolution caused by the flood and the effects of the morphological change on the flood patterns. It is found that the flood leads to scour and the braided form in the middle reach and lower reach, respectively. As a result, the water surface level becomes lower for an upcoming flood event with the same hydrograph, indicating the flood risk considerably decreases in this event. That means, for a fluvial flood with movable bed, the morphological effect is by no means trivial to reliable predict the flood risk. It should be properly taken into account when undergoing the planning, design, construction and management related to flood risk evaluation.

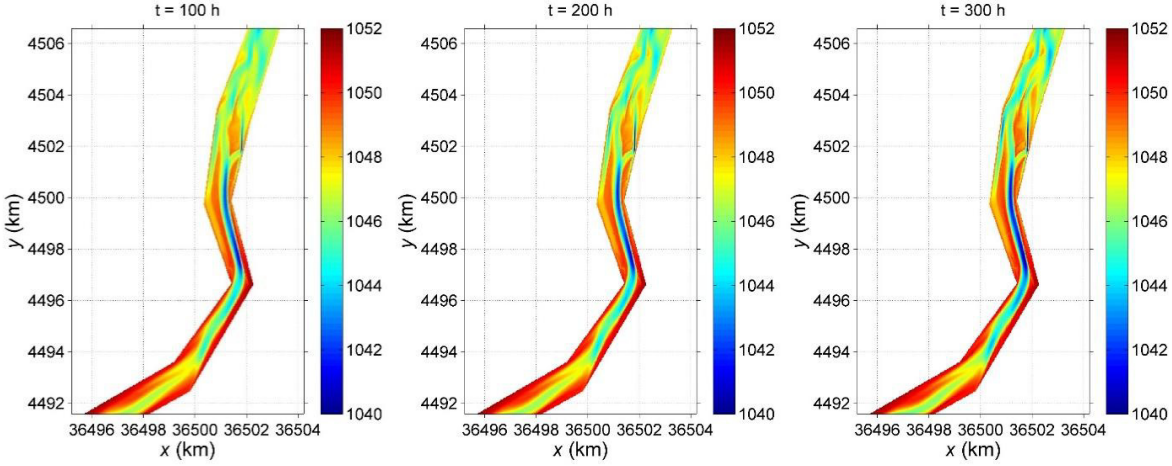

Fig. 8. Computed bed evolution at the Bayangaole Reach of Yellow River for a following flood event.

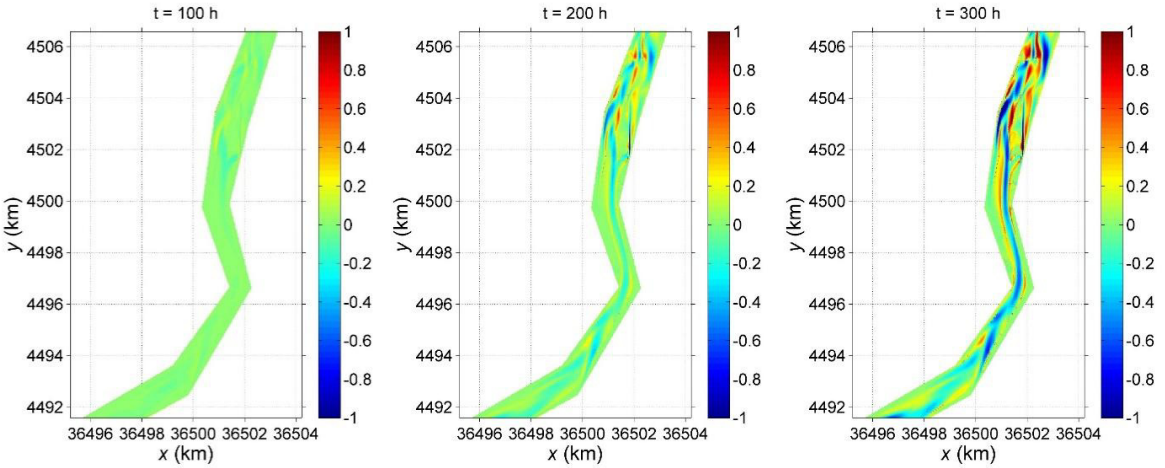

Fig. 9. Computed bed change comparing to the original one at the Bayangaole Reach of Yellow River for a following flood event.

Acknowledgements

This work is partly supported by the State Key Program of National Natural Science Foundation of China (Grant No. 1341330858), UK Engineering and Physical Sciences Research Council (EPSRC) (Grant No. EP/K013513/1) and the UK Natural Environment Research Council (NERC) (Grant No. NE/K008781/1).

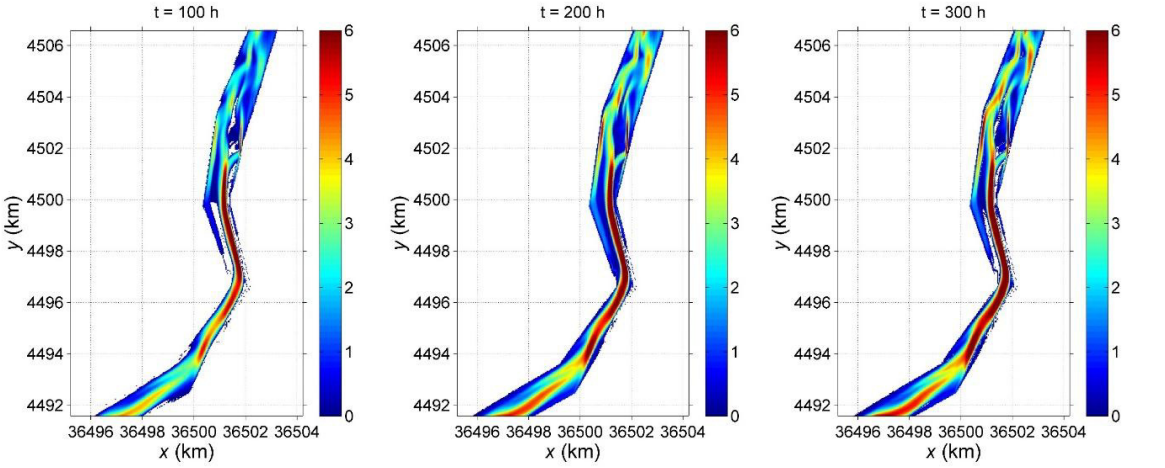

Fig. 10. Computed water depth evolution over the movable bed at the Bayangaole Reach of Yellow River for a following flood event.

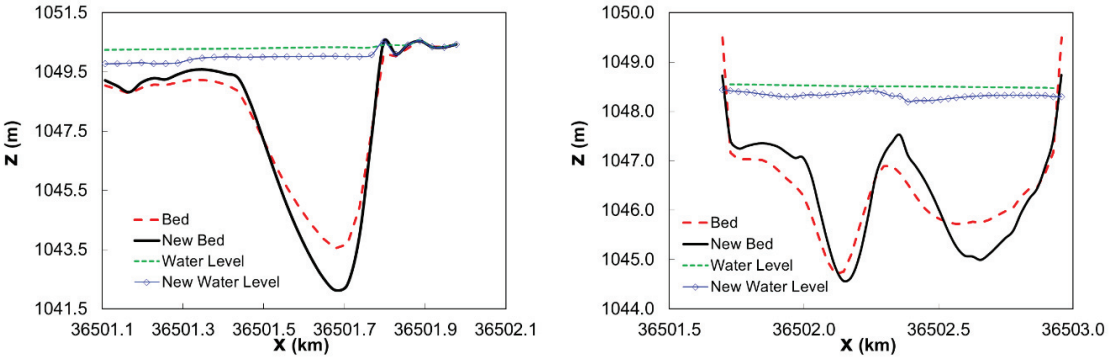

Fig. 11. Comparison between the water level and the river bed at Section 2 (left) and 4 (right) at t = 200 h for the two flood events (New herein means the following flood event).

References

[1] L. Song, J. Zhou, J. Guo, Q. Zou, Y. Liu, A robust well-balanced finite volume model for shallow water flows with wetting and drying over irregular terrain, Advances in Water Resources 34(2011) 915–932.

[2] F. Simons, T. Busse, J. Hou, I. Özgen, R. Hinkelmann, A model for overland flow and associated processes within the Hydroinformatics Modelling System, Journal of Hydroinformatics 16(2014) 375–391.

[3] Q. Liang and L.S. Smith, A high-performance integrated hydrodynamic modelling system for urban flood simulations, Journal of Hydroinformatics 17(2015) 518–533.

[4] M. Guan, N. Wright, P. Andrew Sleigh, Multimode morphodynamic model for sediment-laden flows and geomorphic impacts, Journal of Hydraulic Engineering 141(2015) 04015006-1-12.

[5] J.D. Smith, S.R. McLean, Spatially averaged flow over a wavy surface, Journal of Geophysical Research-Oceans and Atmospheres 82(1977)1735–46.

[6] J. Hou, F. Simons, R. Hinkelmann, A 2D well-balanced shallow flow model for unstructured grids with novel slope source treatment, Advances in Water Resources 52(2013) 107–131.

[7] J. Hou, Q. Liang, F. Simons, R. Hinkelmann, A stable 2D unstructured shallow flow model for simulations of wetting and drying over rough terrains, Computers & Fluids 82(2013) 132–147.

[8] Q. Liang, F. Marche, Numerical resolution of well-balanced shallow water equations with complex source terms, Advances in Water Resources 32(2009) 873–884.

[9] L. Goutiere, S. Soares-Frazão, Y. Zech, Dam-break flow on mobile bed in abruptly widening channel: Experimental data, Journal of Hydraulic Research 49(2011) 367–371.